Mercury-mediated cross-resistance to tellurite in Pseudomonas spp. isolated from the Chilean Antarctic territory

Journal:	*Metallomics*
Manuscript ID	MT-ART-10-2015-000256.R1
Article Type:	Paper
Date Submitted by the Author:	30-Oct-2015
Complete List of Authors:	Rodríguez, Fernanda; Universidad de Santiago de Chile, Díaz, Waldo; Universidad San Sebastián , ; Universidad de Santiago de Chile, Undabarrena, Agustina; Universidad Técnica Federico Santa María, Muñoz, Pablo; Universidad de Santiago de Chile, Arenas, Felipe; Universidad de Santiago de Chile, Biología Vasquez, Claudio; Universidad de Santiago de Chile,

Metallomics

Paper

Mercury-mediated cross-resistance to tellurite in *Pseudomonas* spp. isolated from the Chilean Antarctic territory

F. Rodríguez-Rojas [a], W. Díaz-Vásquez [a-b], A. Undabarrena [c], P. Muñoz-Díaz [a], F. Arenas [a] and C. Vásquez [a]

Mercury salts and tellurite are among the most toxic compounds for microorganisms on Earth. Bacterial mercury resistance is established mainly via mercury reduction by *mer* operon system. However, specific mechanisms underlying tellurite resistance are unknown to date. To identify new mechanisms for tellurite detoxification we demonstrate that mercury resistance mechanisms can trigger cross-protection against tellurite to a group of *Pseudomonads* isolated from the Chilean Antarctic territory. Sequencing of 16S rRNA of four isolated strains resulted in the identification of three *Pseudomonads* (ATH-5, ATH-41 and ATH-43), and a *Psychrobacter* (ATH-62) bacteria species. Phylogenetic analysis showed that ATH strains were related to other species previously isolated from cold aquatic and soil environments. Furthermore, the identified *merA* genes were related to *merA* sequences belonging to transposons commonly found in isolated bacteria from mercury contaminated sites. *Pseudomonas* ATH isolates exhibited increased tellurite resistance only in the presence of mercury, especially ATH-43. Determination of growth curves, minimal inhibitory concentrations and growth inhibition zones showed different tellurite cross-resistance of the ATH strains and suggested a correlation with the presence of *mer* operon. On the other hand, reactive oxygen species levels decreased while thiol content increased when the isolates were grown in the presence of both toxicants. Finally, qPCR determinations of *merA*, *merC* and *rpoS* transcripts from ATH-43 showed a synergic expression pattern upon combined tellurite and mercury treatments. Altogether, the results suggest that mercury could trigger a cell response that confers mercury and tellurite resistance, and that the underlying mechanism participates in protection against oxidative damage.

Introduction

Certain heavy metals and metalloids are harmful for most microorganisms even at very small concentrations.[1-3] Among them, mercury (II) and tellurite exhibit very low minimal inhibitory concentrations (MIC) for *E. coli*.[4, 5] Both toxicants generate cell damage mainly by thiol depletion, enzyme inactivation and oxidative stress.[6-10] Bacterial mercury resistance lies mainly on the MerA flavoenzyme, which transforms toxic Hg^{+2} to the volatile and less toxic elemental mercury.[11] On the other hand, specific mechanisms for detoxifying tellurite have not been reported so far. However, it has been shown that some metabolic flavoenzymes such as dihydrolipoamide dehydrogenase, tiorredoxin reductase and glutathione reductase are able to reduce tellurite to the less-toxic elemental tellurium.[12-14] In addition, an enhanced response to oxidative stress can confer tellurite resistance in some bacteria.[15]

Several studies have demonstrated that sites polluted with heavy metals and/or metalloids contain bacterial species that cope with the toxicity of most metals through different molecular mechanisms, either by direct resistance or by conferring cross-resistance to a wide variety of toxicants. In this line, some naturally occurring examples are *Pseudomonas putida* SP1[16], *Raoultella planticola*[17] and *Cupriavidus metallidurans* CH34[4, 18, 19] which are considered as multimetal-resistant bacteria. In this context, it has been evidenced that common resistance mechanisms to heavy metals have been developed during bacterial evolution. Such is the case of the *czc* system, which is used by some bacteria for detoxifying cadmium, zinc and cobalt.[20] Also, previous studies demonstrated that the *ars* operon, involved in arsenate and arsenite resistance, increases up to 60-fold the MIC of tellurite for *E. coli*.[21] On the other hand, more recently it was observed that the tellurite resistant determinant *trgB*, from the *trgAB* operon, confers copper resistance in *Rhodobacter capsulatus* by a still undetermined mechanism.[22]

In the last century and mainly because of the industrial revolution, it became evident the dramatic increase of heavy metals/metalloids-polluted sites across the Earth surface, including pristine places such as Antarctica.[23, 24] The Antarctic continent is constantly exposed to diverse abiotic stresses such us low temperatures, high salinity, and UV radiation, among others, which can cause oxidative stress in living organisms. Moreover, mercury

[a.1]*Laboratorio de Microbiología Molecular, Facultad de Química y Biología, Universidad de Santiago de Chile, Alameda 3363, Santiago, Chile.*
[b] *Facultad de Ciencias de la Salud, Universidad San Sebastián, Lota 2465, Santiago, Chile.*
[c] *Laboratorio de Microbiología Molecular y Biotecnología Ambiental, Facultad de Química, & Centro de Biotecnología Daniel Alkalay Lowitt, Universidad Técnica Federico Santa María, Av. España 1680, Valparaíso, Chile.*

levels have increased in Antarctica mostly because of the grasshopper effect and mercury depletion events (MDEs).[25, 26] Hence, the Antarctic continent has become an interesting place for sampling and isolating bacterial strains that are resistant to multiple stresses, including that produced by heavy metals.[27] In this context, mercury-resistant bacteria have been isolated from several polar environmental samples.[28] Furthermore, our laboratory identified and characterized, for the first time, highly tellurite resistant psychrotolerant bacteria from Antarctic samples. [29]

The understanding of the molecular mechanisms underlying mercury and tellurite resistance, and the oxidative damage associated to these psychrotolerant bacteria, could allow the design of new bioremediation strategies for polluted places at low temperatures. In this work, psychrotolerant bacteria from the Chilean Antarctic territory showing resistance to mercury and tellurite were analyzed. Some of them are resistant to tellurite only in the presence of mercury, suggesting that this metal could trigger a molecular response that confers cross-resistance to both tellurite and mercury.

Experimental

Bacterial isolation

All samples were collected during the Chilean Antarctic Expedition ECA-48, sponsored by Instituto Antártico Chileno (INACH), 2012. Bacterial strain ATH-5 was isolated from the Collins Glacier (73° 41' S; 65° 55' E), ATH-41 and ATH-43 from Greenwich Island (62° 30' S; 59° 39' W), and ATH-62 from Deception Island (62° 55' S; 60° 37' W), all located in the Antarctic peninsula. For bacterial enrichment, volumes of 100 µL of each sample were suspended in 1 mL of LB media supplemented with amphotericin B 2.5 µg/mL to inhibit fungal proliferation, and incubated for 16 h at room temperature. Then, 60 µL of each culture were spread on LB agar plates containing 40 µM $HgCl_2$ and 40 µM K_2TeO_3, and incubated at 25 °C for 48 h. Pure isolates were obtained by repeated streaking and preserved in 15% glycerol stocks at -80°C. To determine the optimal growth temperature, the isolates were grown individually at 4, 25 and 37 °C.

16S rRNA sequencing and detection of *merA* in the Antarctic strains

For 16S rRNA sequencing, colony PCR was carried out using GoTaq®DNA Polymerase Master Mix (Promega) and universal 16S primers 8F [7] and 1492R [30] at 55 °C (annealing temperature). PCR products were sequenced (Macrogen®) and subjected to nBLAST analysis against bacterial 16S rRNA sequences of the National Center for Biotechnology Information (NCBI) database to determine

strain genus. The *merA* gene was identified in ATH strains by PCR using purified genomic DNA as template and universal specific primers for the *mer* operon (Forward P1: GGCTATCCGTCCAGCGTCAA, and Reverse A5: ACCATCGTCAGGTAGGGGACCAA) as described by Felske *et al*.[31] The PCR consisted in 30 cycles that included a denaturation step at 95 °C for 30 s, annealing at 60 °C for 30 s and extension at 72 °C for 2 min. PCR products were sequenced (Macrogen®) and then subjected to nBLAST. The sequenced products allowed determining the start codon of *merA* sequences to design forward primers for all analyzed *merA* genes. For designing reverse primers for *merA* encoding open reading frames, sequences of the first hits of the nBLAST analysis were used. ATH-5, ATH-41 and ATH-43 *merA* cloning included start codon and excluded stop codons in each case. Primer sequences for ATH-43 were: forward 5'-ATGACCGAACTGAAAATCATTG-3' and reverse 5'-CCCCCCTGCGCAGCA-3'(designed from *Pseudomonas putida* SP1, accession N° ADJ53344); for ATH-41: forward 5'-ATGACTGAATTGCAAATCGTTGG -3' and reverse 5'-GCCGGCGCAGCAGGAAAG-3'(designed from *Xanthomonas campestris*, accession N° Y17691); for ATH-5: forward 5'-ATGACTACTCTGCAAATCAGC-3' and reverse the same as for ATH-41. PCR was the same as for P1-A5 primers, except for the annealing temperature was 55 °C. All PCR products were sequenced (Macrogen®) to obtain the complete open reading frames of each *merA* gene.
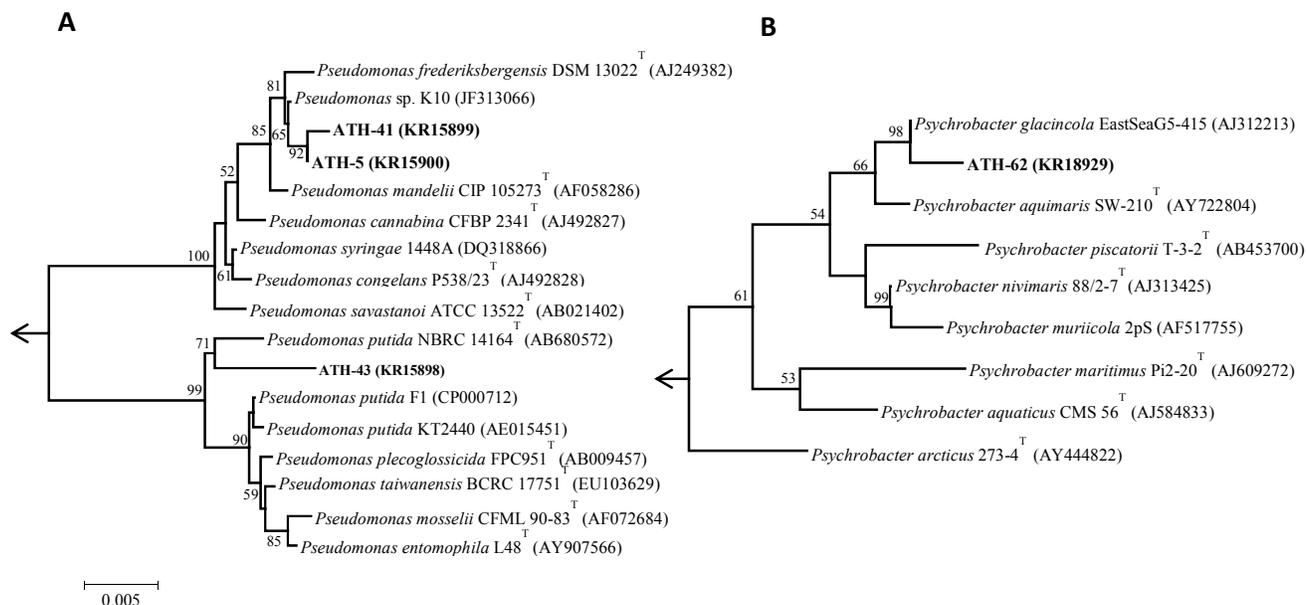
Phylogenetic trees

Almost complete sequences of the 16S rRNA genes and *merA* ORFs (translated sequence) were used to construct phylogenetic trees. To obtain almost complete sequences of each 16S rRNA gene, PCR products previously amplified were additionally sequenced with universal primers 518F and 800R (Macrogen®). Sequence edition, alignment and contigs analysis were carried out using the Vector NTI v10 software package (Invitrogen). Contigs were evaluated by nBLAST against 16S ribosomal RNA sequences of the Bacteria and Archaea databases to establish the closest type strain match, and Nucleotide Collection Databases (NCBI), to search for other phylogenetically related organisms. Construction of phylogenetic trees was based on the V1-V9 region of 16S rRNA gene sequences using the Neighbor Joining Algorithm [32] and for the *merA* tree Maximum-likelihood algorithm, with bootstrap values of 1000 replications [33] and MEGA software version 6.0[34]. The 16S rRNA and *merA* sequences of ATH strains were deposited in GenBank under the following accession numbers: KR15900 (16S rRNA_ATH-5), KR15899 (16S rRNA_ATH-41), KR15898 (16S rRNA_ATH-43), KR18929 (16S rRNA_ATH-62), KR818931 (*merA*_ATH-5), KR827601 (*merA*_ATH-41), and KR818930 (*merA*_ATH-43).

Table 1. Geographical and phenotypic characteristics of the ATH strains

Strain	Isolation site	Optimal growth Temperature (°C)	Closest type strain (% identity)	Most closely related *merA* (species,% identity)
ATH-5	Collins Glacier	20-25	*Pseudomonas mandelii* CIP 105273[T] (99,65%)	Tn5044 (*Xanthomonas campestris,* 98.03%)
ATH-41	Prat base, Greenwich Island	20-25	*Pseudomonas mandelii* CIP 105273[T] (99,43%)	Tn5044 (*Xanthomonas campestris,* 86.96%)
ATH-43	Prat base, Greenwich Island	20-37	*Pseudomonas putida* NBRC 14164[T] (99,77%)	Tn5041 (*Pseudomonas putida* DLL-E4, 99.76%)
ATH-62	Péndulo cove, Deception Island	20-25	*Psychrobacter aquimaris* SW-210[T] (99,50%)	ND

ND = Non determine

A

B

Fig. 1 Phylogenetic tree of the Antarctic isolates. Neighbor-joining tree of 16S rRNA gene sequences. Node numbers represent the percentage of bootstrap replicates of 1000 resamplings (values below 50% are not shown). A, phylogenetic tree for isolates ATH-5, ATH-41 and ATH-43. B, phylogenetic tree for ATH-62. Positions 28-1447 and 31-1452 of gene sequence were considered according to the *E. coli* K12 16rRNA gene sequence, for *Pseudomonas* and *Psychrobacter* trees, respectively. Scale bar represents 0.005 substitutions per nucleotide positions. Arrow points to the outgroup *E. coli K12* (AP012306). All accession numbers are in parenthesis following the bacterial strain.

Antibiotic susceptibility and biochemical characterization

For antibiotic susceptibility analysis, cells were grown to exponential phase and spread onto Mueller-Hinton agar plates. Antibiotic displays for Gram (-) bacteria (Valtek®) were used and growth inhibition zone diameters were measured and compared with values from the Clinical and Laboratory Standards Institute (CLSI) to determine susceptibility or resistance to each tested antibiotic.

For biochemical characterizations, analytical profile indexes (API®) were used according to manufacturer instructions.

Growth curves, growth inhibition zones and MIC determinations

Minimal inhibitory concentrations (MIC) of K_2TeO_3 and $HgCl_2$ were determined in LB media supplemented with increasing concentrations of the respective toxicants. Cultures were started with 1:100 dilutions of saturated cultures. To determine the MIC of K_2TeO_3 in the presence of $HgCl_2$, all cultures contained $HgCl_2$ at a concentration equivalent to ¼ of the MIC (determined previously for each strain) and increasing concentrations of K_2TeO_3. For growth curves construction, cells were inoculated in LB broth using 1:100 dilutions of overnight cultures and subjected to the following conditions: 1 MIC of K_2TeO_3, ¼ MIC of $HgCl_2$, and both toxicants combined at the same concentrations, at 25 °C for 15 h. Optical density at 600 nm was monitored using a microplate multireader Tecan Infinite® 200 PRO.

To determine growth inhibition zones, ATH cells grown to OD_{600} ~ 0.3 were seeded onto LB agar plates supplemented or not with $HgCl_2$ (¼ MIC for the respective strain) and sterile circular paper discs embedded with 10 μL of K_2TeO_3 400 mM were placed at the centers of the plates. Plates were incubated at 25 °C for 48 h.

Reactive oxygen species and thiol quantification

Reactive oxygen species (ROS) were determined using the oxidant-sensitive probe 2',7'-dichlorodihydrofluorescein diacetate (H_2DCFDA, Sigma-Aldrich) essentially as described by Pérez *et al.*[8] Briefly, cultures were grown to OD_{600} ~ 0.3 and treated either with ¼ MIC of $HgCl_2$, ½ MIC of K_2TeO_3 or simultaneously with both toxicants at the same concentration at 25 °C for 30, 60 and 90 min. Measurements were carried out after each treatment by exciting the probe at 490 nm and measuring the fluorescence intensity at 519 nm with a microplate multireader Tecan Infinite® 200 PRO. Fluorescence intensity values were normalized by OD_{600}.

Thiol content was quantified by Ellman's method using 5,5'-dithiobis-(2-nitrobenzoic acid)(DTNB, Sigma-Aldrich), as previously described by Turner *et al.*[7] Experimental conditions were the same as for ROS determination. TNB^{-2} absorbance was measured spectrophotometrically at 412 nm (extinction coefficient of 13600 $M^{-1}cm^{-1}$). A standard curve of reduced glutathione was constructed for assay calibration. Data values were normalized by protein concentration as determined by the Bradford method.[35]

All experiments were performed in triplicate and Student's t-test was applied for statistical analysis when required.

RNA purification and Real Time PCR

For RNA isolation, ATH-43 was grown to OD_{600} ~ 0.3 and treated with mercury, tellurite or both toxicants for 10 min at the same concentrations as for ROS and thiols quantification. Briefly, cells were harvested and RNA was isolated using the Favorprep tissue total RNA purification mini Kit (Favorgene). RNA quantification was carried out by using Quant-it Ribogreen Kit (Invitrogen), following the instructions of the manufacturer. Quantitative PCR was conducted using a Light Cycler 1.5 thermocycler with the RNA MasterSYBR Green Kit (Roche Applied Science). Real time PCR

program involved reverse transcription at 40 °C for 10 min, followed by 45 cycles of denaturation at 95 °C for 30 s; annealing at 55 °C for 30 s, and extension 72 °C, 30 s. Specific primers for *merA* amplification (forward 5'-GTTCCACCGATTCCAGGACTG-3'; reverse 5'-CAGTACGAACTCGCCGTTGG-3'), *merC* (forward 5'-TTTCCCGCCCTTGCTAGTCT-3'; reverse 5'-ATGAGCGGGCGACACGAGAT-3') and *rpoS* (forward 5'-TAAAGAAGTGCCGGAGTTTGACA-3'; reverse 5'-TTGCTTTCGATCATGCGCTT-3') from ATH-43 were used. The D-glyceraldehyde-3-phosphate dehydrogenase gene, *gapA* (forward 5'-CCAGTGTCTTGGTGAGTGGATTG;-3'; reverse 5'-CCATTGCCTTCCTGCTTGA-3'), and the 16S rRNA gene (forward 5'-GATTCCAACGGCTAGTTCACATC-3'; reverse 5'-GGTGCAAGCGTTAATCGGAA-3') were used as reference genes for normalization. All transcript levels were calculated using the ΔΔCt method.[36]

Results

Identification and characterization of mercury and tellurite-resistant bacteria from Antarctica

Of nineteen Antarctic samples analyzed, four bacterial isolates named ATH strains (Table 1) exhibiting simultaneous resistance to mercury and tellurite were obtained. While ATH-5 was isolated from a sample collected at Glacier Collins (King George Island), ATH-41 and ATH-43 were from soil samples at the Chilean Prat military base (Greenwich Island). In turn, ATH-62 was obtained from Péndulo Cove, Deception Island, a location that was devastated by a volcanic eruption in 1964. All strains were Gram (-) and grew optimally between 20 and 25 °C, excepting ATH-43, which grew between 20 and 37 °C. The 16S rRNA sequence data revealed that ATH-5, ATH-41 and ATH-43 belonged to the *Pseudomonas* genus, whereas ATH-62 was related to the *Psycrobacter* genus. Further comparisons with 16S sequences from NCBI, showed that the closest type strains were *Pseudomonas mandelii* CIP 105273[T] for ATH-5 and ATH-41, *Pseudomonas putida* NBRC 14164[T] for ATH-43, and the halophilic bacteria *Psychrobacter aquimaris* SW-210[T 37] for

ATH-62. Phylogenetic trees based on the almost complete 16S rRNA gene sequences showed that ATH-5 and ATH-41 were also related to *Pseudomonas frederiksbergensis* DSM 13022[T 38] and to *Pseudomonas* sp. K10, while ATH-43 phylogeny was related to various *Pseudomonas putida* species (Fig. 1A) and ATH-62 to *Psychrobacter glacincola* EastSeaG5-415 (Fig. 1B).

Antibiotic susceptibility tests for Gram (-) bacteria determined that while ATH-5, ATH-41 and ATH-43 were resistant to almost all antibiotics (except for amikacin, gentamicin and ciprofloxacin); ATH-62 was sensitive to all of them (Supplementary Table 1). The biochemical characteristics of ATH-5, ATH-41 and ATH-43 were very similar, unlike ATH-62 which used all the tested carbon sources (Supplementary Table 2).
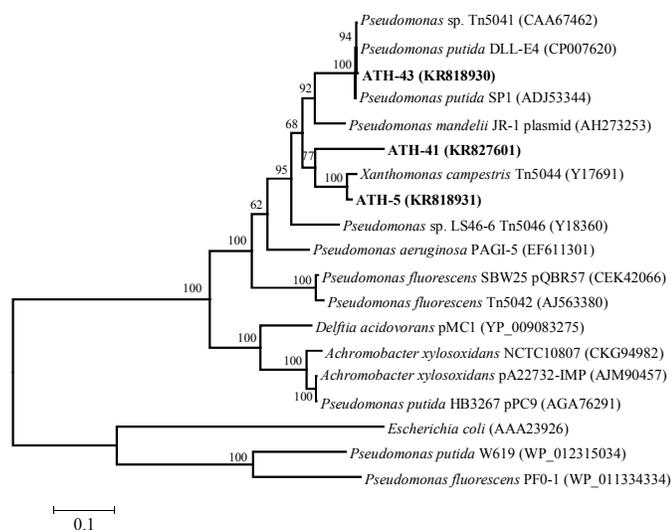
To identify *mer* operons, universal primers that amplify a specific operon sequence including part of the 3' end of *merP* and part of the 5' of *merA* gene were used. The mer operon was detected in ATH-5, ATH-41 and ATH-43 utilizing primers P1 and A5 (see Experimental) (Table 1). Even though several set of primers were utilized as described in [31] *mer* operon was not found in ATH-62 (not shown). The P1-A5 sequences determined for ATH-5, ATH-41 and ATH-43 were used to design specific primers to amplify complete *merA* sequences. BLAST analysis showed that *merA* from ATH-5 and ATH-41 was related to that of transposon Tn5044 found in *Xanthomonas campestris* (Table 1). On the other hand, *merA* from ATH-43 exhibited high identity with *merA* from *Pseudomonas putida* DLL-E4 transposon Tn5044 (Table 1). Phylogenetic tree constructed with *merA* sequences showed that *merA* genes from ATH isolates were phylogenetically related mainly to sequences found in transposable elements (Tn5041, Tn5044 and Tn5046) from different *Pseudomonas* species isolated from several environments (Fig. 2).

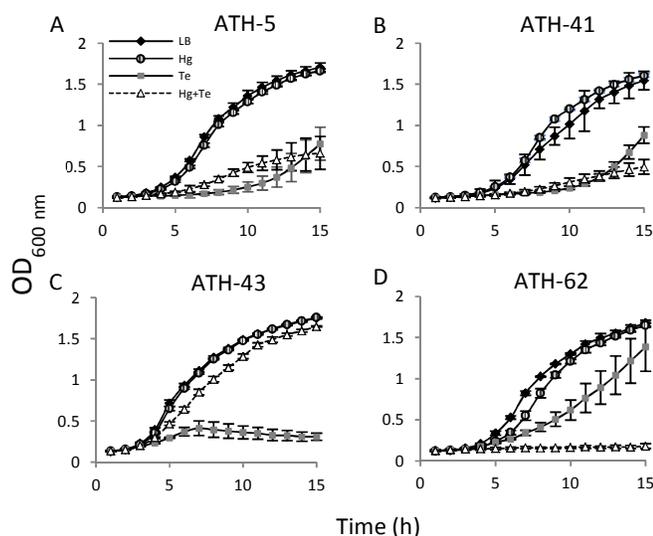### Mercury enhances tellurite resistance in *Pseudomonas* spp. isolated from Antarctica

Preliminary experiments carried out in our laboratory showed that the ATH-43 isolate grew in the presence of tellurite up to 40 μM only if the cultures were supplemented with sublethal mercury concentrations (~ 40 μM). This observation prompted us to assess if mercury caused the same phenotype in the other isolates. While ATH-43 showed the highest and lowest MICs of mercury (HgMIC) and tellurite (TeMIC), respectively, ATH-5 and ATH-41 exhibited almost similar sensitivity to both toxicants. On the other hand, and although exhibiting a rather similar HgMIC regarding the other strains, ATH-62 showed the highest resistance to tellurite (Table 2). To assess if mercury can induce resistance to tellurite in ATH strains, the TeMIC was determined in the presence of mercury. The results showed that it increased 8,3-fold in ATH-43 when compared to the tellurite treatment alone. TeMIC increased 1,5-fold in ATH-5, while it remained unaltered in ATH-41. In contrast, it decreased 2,3-fold for ATH-62 in the presence of mercury (Table 2).

Fig. 2 Phylogenetic tree of *merA* from ATH-5, ATH-41 and ATH-43. Maximum-likelihood tree of *merA* (translated nucleotide sequence); node numbers represent the percentage of bootstrap replicates of 1000 resamplings (values below 50% are not shown). The tree was rooted with the paralog enzyme glutathione reductase (GOR) from three different species. Scale bar represents 0.01 substitutions per nucleotide positions. All accession numbers are shown in parenthesis

Table 2. Minimal inhibitory concentrations of mercury, tellurite and tellurite in the presence of mercury

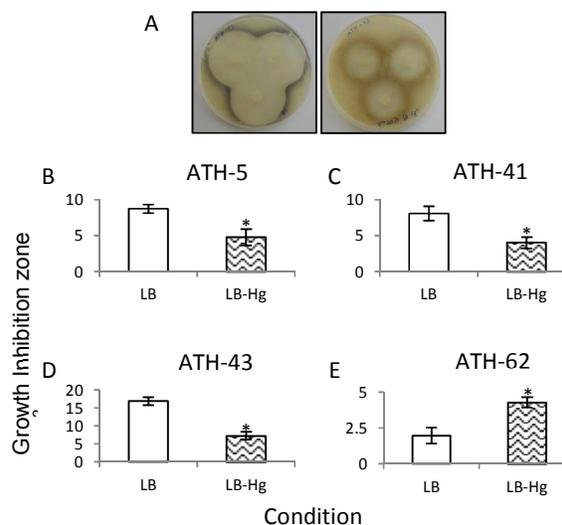| Strain	Hg^{+2} (μM)	TeO_3^{-2} (μM)	TeO_3^{-2} (μM) w/ Hg^{+2}
ATH-5	100	80	120
ATH-41	100	120	120
ATH-43	200	24	200
ATH-62	80	700	300

Fig. 3 Growth curves of the Antarctic strains. ATH-5 (A), ATH-41 (B), ATH-43 (C) and ATH-62 (D) growth was monitored at OD$_{600nm}$ for 15 h in four different conditions each one: control (black rhomboid), mercury treatment (striped circle), tellurite treatment (grey square) and mercury/tellurite treatment (white triangles). All curves are shown as the mean ± SD of three independent experiments.

Fig. 4 Determination of growth inhibition zones. The ATH strains were grown in LB plates supplemented or not with mercury, and growth inhibition zones were measured after 24 h at 25 °C around the central tellurite-containing disc. A, halos in LB agar plates showing ATH-43 grown in the presence (right) or absence (left) of mercury. The growth inhibition zones of ATH-5 (B), ATH-41 (C), ATH-43 (D) and ATH-62 (E) are shown as the mean ± SD of three independent experiments. Asterisks represent p values < 0.05.

Then growth curves were constructed in four different conditions: no toxicant amended (controls), mercury, tellurite, and combined mercury/tellurite treatments (Fig. 3). Growth curves of ATH-5 and ATH-41 were similar for all treatments (Fig. 3A and 3B). They grew as fast as the control in the presence of mercury, but tellurite and mercury/tellurite treatments delayed drastically bacterial growth, with a slight increase of ATH-5 growth in the presence of mercury/tellurite (Fig. 3A). On the other hand, mercury alone did not alter ATH-43 growth, and as expected, tellurite amendment inhibited growth rapidly (Fig. 3C). Interestingly, the combined mercury/tellurite treatment almost did not affect ATH-43 growth, which was similar to that observed in control and mercury-amended cultures. In contrast to the results observed with the *Pseudomonads* isolates, ATH-62 showed delayed growth with tellurite and a total growth inhibition in the presence of both toxicants.

In a third approach to characterize the potentiation of tellurite resistance phenotype by mercury, tellurite growth inhibition zones were determined in the presence and absence of mercury (Fig. 4). As shown before, ATH-43 exhibited the most evident potentiation effect on tellurite resistance. In fact, the growth inhibition zone decreased 2.5 fold in the presence of mercury (Fig. 4A and 4D). In turn, ATH-5 and ATH-41 exhibited a slight but significant growth decrease in mercury amended medium (Fig. 4B and 4C). The opposite effect was observed with ATH-62, i.e., the growth inhibition zone increased 2.19 fold in the presence of mercury as compared to controls (Fig. 4E).

Altogether, these results suggest that mercury potentiates tellurite resistance in the Antarctic *Pseudomonads* isolates, especially ATH-43, but not in *Psychrobacter sp.* ATH-62.

ROS and thiol content in Antarctic isolates exposed to mercury and tellurite

It has been previously demonstrated that both, mercury and tellurite, induce ROS production [3, 10] and that also show strong affinity for sulfhydryl containing molecules.[7, 39] In this context, ROS levels were quantified in terms of fluorescence intensity under the same experimental conditions described above for ATH strains (see Experimental for details) (Fig. 5). ATH-5 and ATH-41 produced low and rather constant ROS in the absence of toxicant amendment, while toxicant exposure raised ROS levels significantly (Fig. 5A and 5B). Mercury and mercury/tellurite treatments showed a trend to decrease ROS levels after 30 min of toxicant exposure, increasing afterwards. This was observed in tellurite-exposed ATH-41, but not in ATH-5, where ROS levels exhibited a constant increase (Fig. 5A and 5B). Interestingly, ATH-43 showed higher ROS levels with tellurite in comparison to mercury and mercury/tellurite exposure (Fig. 5C). Nevertheless, it showed a marked tendency to reduce ROS levels in all metal treatments, almost reaching the ROS content observed in the control condition with mercury and mercury/tellurite treatments (Fig. 5C). Conversely to *Pseudomonas* strains results, ATH-62 behaved differently regarding ROS production (Fig. 5D). Tellurite did not affect significantly ROS levels as compared to control treatments. However, mercury and mercury/tellurite exposure resulted in augmented ROS levels (Fig. 5D). These results show that tellurite enhances ROS production in the *Pseudomonas* isolates, but when combined with mercury a reduction of ROS levels is observed, especially in ATH-43. In the case of ATH-62, a distinct response was evidenced, where mercury did not favor a ROS level decrease in the combined mercury/tellurite treatment.

Given the ability of tellurite and mercury to interact with reduced thiols, the RSH content was analyzed (Fig. 6) The RSH content decreased drastically in ATH-5 during all treatments and did not recover the initial levels after 90 min (Fig. 6A). Although there was
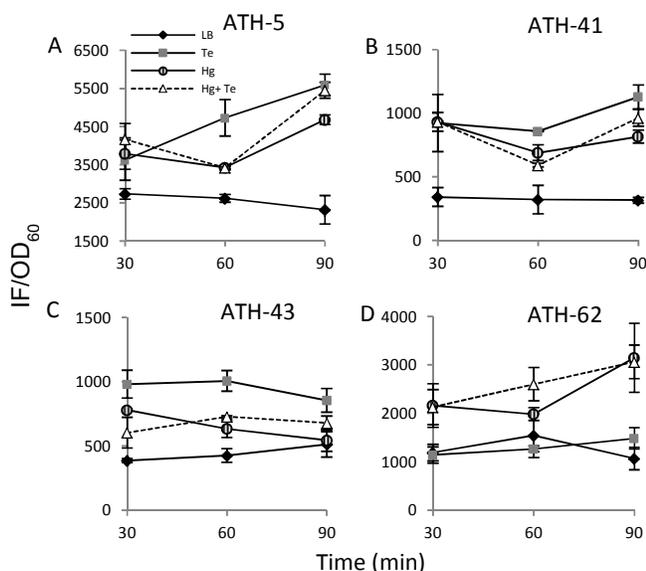
Fig. 5 Quantification of reactive oxygen species (ROS) in the Antarctic strains. Cells grown to $OD_{600nm} \sim 0.3$ were exposed to mercury (striped circle), tellurite (grey square), mercury/tellurite (white triangles). Controls were not exposed to toxicants (black rhomboid). ROS content in ATH-5 (A), ATH-41 (B), ATH-43 (C) and ATH-62 (D) was assessed spectrophotometrically at 519 nm at 30, 60 and 90 min exposure. Plots are shown as the mean ± SD of three independent experiments, p< 0.05.

also a decrease of RSH levels in ATH-41, a general trend to recover them over time was observed (Fig. 6B). ATH-43 also showed an initial reduction of thiols content that in the case of the combined treatment recovered to that exhibited by controls up to 90 min exposure (Fig. 6C). ATH-62 showed a similar response to that observed for ATH-5 where thiol content decreased after the treatments and remained at low concentrations.

**Expression analysis in response to mercury and tellurite in ATH-43**

To shed light on the molecular mechanism(s) underlying the mercury-triggered potentiation of tellurite resistance the expression of three selected genes of ATH-43 was analyzed (Fig. 7). The expression patterns of two genes belonging to the *mer* operon, *merA* and *merC*, along with the general stress response gene *rpoS* was evaluated after 10 min of toxicant exposure. In general, all three genes were upregulated. The sole exception was *rpoS* where its expression remained unaltered when cells were grown in the presence of mercury. Taken together, qPCR experiments suggest that the combination of mercury and tellurite could generate a synergic effect over the expression of *mer* genes, and probably other genes involved in the general stress response.

Discussion

This work shows that mercury resistance mechanisms from a group of psychrotolerant Antarctic bacteria are involved in tellurite resistance. Four isolates (ATH-5, ATH-41, ATH-43 and ATH-62) were characterized as mercury/tellurite resistant bacteria (Table 1). ATH-5, ATH-41 and ATH-43 were related to *Pseudomonas* species, while ATH-62 was to the *Psychrobacter* genus. Phylogenetic trees showed

that ATH-5 and ATH-41 were related to psychrotrophic *Pseudomonas mandelii* CIP 105273[T] isolated from mineral waters[40] and to the arctic isolate *Pseudomonas* sp. K10 (accession number JF313066) (Fig. 1A). On the other hand, ATH-43 phylogeny was related to *P. putida* isolated from different ecosystems including water and soil polluted sediments[41] (Fig. 1A), while ATH-62 was associated to *Psycrobacter* species isolated from cold environments like permafrost[42], marine ice[43] and Antarctic water[44], among others (Fig. 1B).

The *mer* operon was detected only in the *Pseudomonas* strains. Phylogenetic relationships among *merA* genes from ATH-5, ATH-41 and ATH-43 showed that they were related to *merA* genes found in transposable elements ubiquitous in nature.[45] Even though *merA* from ATH-5 and ATH-41 were related to the *merA* sequence of Tn5044 found in *X. campestris*, *merA* from ATH-41 formed a distinct branch within the phylogenetic tree and could represent a new type of MerA due its low sequence identity with other sequenced *merA* genes (Fig. 2). Moreover, the *mer* operon from ATH-5, and not that from ATH-41, contained the accessory gene *merC*, suggesting that although they are related strains, they do not share the same gene structure of *mer* operon. On the other hand, *merA* from ATH-43 was phylogenetically related to *merA* genes found in other *P. putida* strains that harbor transposon Tn5041, including the multi-metal resistant strain *P. putida* SP1.[16] Tn5041 and Tn5044 are mercury resistance transposons that are considered as dissemination vehicles of mercury resistance in bacterial populations.[46-48] Interestingly, *mer* operon from Tn5044 is expressed exclusively at temperatures below 30 °C.[46, 49] No *mer* sequences were found in ATH-62, suggesting that this bacterium harbors other molecular mechanism(s) to cope with mercury toxicity. In this line, besides the *mer* system, other mercury detoxification mechanisms have been described such as reduction of mercury uptake and mercury ions biosorption by cell surface proteins.[45, 50] Moreover, the *mer* operon-mediated mercury resistance has been associated with
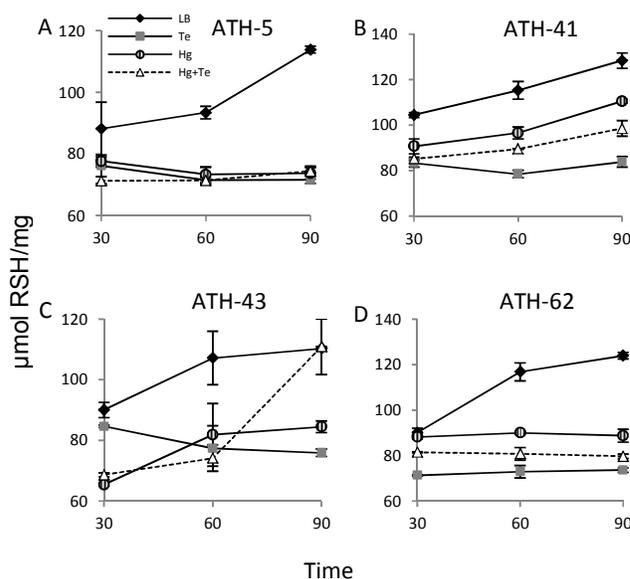
Fig. 6 Thiol content in the ATH Antarctic strains. Cells grown to $OD_{600nm} \sim$ 0.3 were exposed to mercury (striped circle), tellurite (grey square), mercury/tellurite (white triangles). Controls were not exposed to the toxicants (black rhomboid). Thiol quantification of ATH-5 (A), ATH-41 (B), ATH-43 (C) and ATH-62 (D) was assessed spectrophotometrically at 412 nm at 30, 60 and 90 min exposure. Plots are shown as the mean ± SD of three independent experiments, p< 0.05.

antibiotic determinants since genes encoding them are commonly found in mobile genetic elements such as plasmids and transposons.[51] Thus, we hypothesize that the lack of antibiotic resistance observed in ATH-62 may be correlated to the absence of the *mer* operon. Further studies should be performed to understand the molecular nature of mercury resistance and the intrinsic high tellurite resistance displayed by ATH-62.

Through several experimental approaches such as growth curves, MICs, and growth inhibition zone determinations, it was observed that when ATH-5, ATH-41 and ATH-43 were grown in the presence of mercury, their tellurite resistance was increased (Fig. 3, 4 and Table 2). While ATH-5 and ATH-41 showed a weak cross-resistance phenotype, ATH-43 exhibited a strong potentiation of tellurite resistance in the presence of mercury. Conversely, ATH-62 showed a totally opposite response, where the presence of mercury did not favor this phenotype, suggesting that the cross-resistance phenotype could be, at least in part, explained by the presence of *mer* genes.

To date, defining tellurite resistance mechanisms is limited to some studies that establish an involvement of a generalized oxidative stress response[7-9, 52], cysteine metabolism[53-55], volatilization of alkylated tellurium compounds[56], non-enzymatic[7, 52] and enzymatic reduction. Some of the enzymes exhibiting tellurite-reducing activity belong to the flavoprotein family including glutathione reductase[13], tiorredoxin reductase[12], dihydrolipoil dehydrogenase[14], and alkylhydroperoxide reductase. In this context, preliminary results from our laboratory have shown that MerA encoded in the environmental plasmid pTP6 [57], exhibits tellurite reductase activity, suggesting that it could participate in tellurite reduction (unpublished data). In support of this, recently, Marteyn *et al.* observed that purified mercuric reductase from *Synechocystis* PCC6803 can reduce uranyl cations thus breaking the paradigmatic specificity of MerA for mercuric ions.[58]

To study the molecular response associated with the observed potentiation phenomenon, the reactive oxygen species content was analyzed. It was found that both tellurite and mercury elicited ROS production in all *Pseudomonas* strains, but not in ATH-62 (Fig. 5). It is well documented that tellurite induces superoxide formation during its reduction to elemental tellurium in several bacterial species.[8, 9, 29] Since ATH-62 displayed the highest tellurite MIC, it

Fig. 7 Real time PCR for *merA*, *merC* and *rpoS* from ATH-43. Gene expression of *merA* (rhomboids), *merC* (squares) and *rpoS* (triangles) was determined by the ΔΔCt method from RNA samples obtained from ATH-43 cultures treated with mercury, tellurite and mercury/tellurite. Plot is shown as the mean ± SD of three independent experiments, p< 0.05.

may harbor specific tellurite resistance determinants that could be involved in controlling ROS production or detoxification in toxicant-exposed cells. ATH-43 was the only strain that reduced ROS levels up to those observed in control conditions, suggesting that it may possess stronger molecular mechanism(s) that can cope with oxidative stress which would be induced solely in the presence of mercury. Proteomic analysis carried out in *E. coli* and *Corynebacterium glutamicum* have shown that mercury triggers molecular responses against oxidative stress such as over-production of superoxide dismutase, cysteine synthase, tiorredoxin reductase and glutathione reductase, among others.[10, 59] Hence, ATH-43 may contain specialized molecular determinants involved in the oxidative stress response which would be strongly elicited by mercury. These mechanisms could be complementary to the *mer* detoxification system, and as consequence, also useful for tellurite detoxification.

Both mercury and tellurite decreased the thiol content in all ATH strains (Fig. 6). Hg^{+2} displays the highest affinity for sulfhydryl groups in nature among heavy metals, and thus its toxicity occurs principally due to oligodynamic effects that causes enzymatic inactivation, thiol depletion and oxidative stress.[11, 60] On the other hand, tellurite is recognized as a strong oxidizing molecule that also produces rapid intracellular thiol depletion in bacteria, especially of glutathione.[7, 39, 52] Interestingly, only ATH-43 showed thiol levels similar to control condition when treated with mercury/tellurite (Fig. 6A). This synergic effect may be a consequence of a tellurite-induced activation of still undefined mechanisms promoting thiol restoration. This phenomenon was not observed when ATH-43 was exposed to other thiol-depleting conditions such as cadmium, copper or chromium. Mercury did not cause a rapid thiol depletion in ATH-62 (Fig. 6D), which could suggest that the mercury resistance phenotype in this strain might be related to a reduction of mercury uptake, as occurs in the lactic acid bacteria, *Weissella viridescens*.[50]

Finally, tellurite induced the expression of *merA* and *merC* (Fig. 7). It has been previously shown that heavy metals such as cadmium and zinc can activate the expression of the *mer* operon in *Nitrosomonas europaea* by a mechanism that does not involve enzymatic reduction or detoxification of those heavy metals.[61, 62] In this line, it has been suggested that *mer* genes could be considered as putative "sentinel genes", since their expression is highly upregulated in the presence of defined heavy metals and the produced Mer proteins could act as heavy metal chelators.[61, 62] Although tellurite induces *mer* genes expression, this appears to be not enough to confer tellurite resistance. Nevertheless, a synergic effect was again observed in terms of *merA* and *merC* expression after mercury/tellurite exposure. Up-regulation of *merA* could be associated to an increased demand of mercury (and probably tellurite) reduction, whereas the heavy metal transporter, *merC*, could be facilitating the influx of both toxicants thus favoring a rapid detoxification, as occurs with cadmium in the transgenic, *merC*-expressing *S. cerevisiae*.[63] On the other hand, up-regulation of *rpoS* could be a consequence of a multiple stress condition including oxidative stress as evidenced in *E. coli* and *P. aeruginosa* [64, 65], during the so-named cross-protection phenotype.[66]

To date, cross-resistance responses to several toxics have been documented for a number of organisms. Examples include the cadmium-mediated adaptive response conferring cross-protection against high concentrations of hydrogen peroxide and zinc in *X. campestris*. [67, 68] as well as hydrogen peroxide confers cross-resistance to cadmium, mercury and arsenite in Chinese Hamster
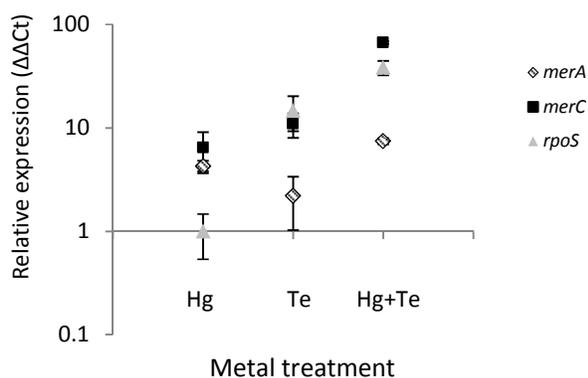
Ovary cells. [69] On the other hand, evolutionary engineering microorganisms have shown several cross-resistance phenotypes. Some examples include the cobalt hyper-resistant *S. cerevisiae*, also displaying high resistance to nickel, zinc and manganese [70] and the boron-resistant *Bacillus boroniphilus*, exhibiting in addition resistance to copper, iron and salt stress. [71] Finally, it was communicated that low tellurite concentrations can induce an adaptive response that results in increased tellurite resistance in *Proteus mirabilis.* [72]

Further experiments are being carried out in our laboratory to better understand the molecular response that underlies the cross-resistance to tellurite induced by mercury in ATH-43 strain.

Conclusions

This work show, for the first time, that the molecular mechanisms underlying bacterial mercury resistance can participate in cross-resistance to tellurite in a group of *Pseudomonas* isolated from Antarctica. As enzymatic reduction is the most familiar tellurite detoxification mechanism and preliminary results from our laboratory suggest that the flavoprotein mercuric reductase (MerA) displays tellurite reduction activity, this enzyme could be responsible of part of the observed tellurite resistance in mercury-resistant bacteria.

Acknowledgements

References

1. J. J. Harrison, H. Ceri, C. A. Stremick and R. J. Turner, *Environmental microbiology*, 2004, **6**, 1220-1227.
2. S. Silver and T. Phung le, *Journal of industrial microbiology & biotechnology*, 2005, **32**, 587-605.
3. J. A. Lemire, J. J. Harrison and R. J. Turner, *Nature reviews. Microbiology*, 2013, **11**, 371-384.
4. M. Mergeay, D. Nies, H. G. Schlegel, J. Gerits, P. Charles and F. Van Gijsegem, *Journal of bacteriology*, 1985, **162**, 328-334.
5. D. E. Taylor, *Trends in microbiology*, 1999, **7**, 111-115.
6. V. B. Mathema, B. C. Thakuri and M. Sillanpaa, *Archives of microbiology*, 2011, **193**, 837-844.
7. R. J. Turner, J. H. Weiner and D. E. Taylor, *Microbiology*, 1999, **145**, 2549-2557.
8. J. M. Pérez, I. L. Calderón, F. A. Arenas, D. E. Fuentes, G. A. Pradenas, E. L. Fuentes, J. M. Sandoval, M. E. Castro, A. O. Elías and C. C. Vásquez, *PLoS ONE*, 2007, **2**, e211.
9. V. Tremaroli, S. Fedi and D. Zannoni, *Archives of microbiology*, 2007, **187**, 127-135.
10. Y. Gao, X. Peng, J. Zhang, J. Zhao, Y. Li, Y. Li, B. Li, Y. Hu and Z. Chai, *Metallomics*, 2013, **5**, 913-919.
11. T. Barkay, S. M. Miller and A. O. Summers, *FEMS microbiology reviews*, 2003, **27**, 355-384.
12. M. P. Rigobello, A. Folda, A. Citta, G. Scutari, V. Gandin, A. P. Fernandes, A. K. Rundlof, C. Marzano, M. Bjornstedt and A. Bindoli, *Free radical biology & medicine*, 2011, **50**, 1620-1629.
13. B. Pugin, F. A. Cornejo, P. Muñoz-Díaz, C. M. Muñoz-Villagrán, J. I. Vargas-Pérez, F. A. Arenas and C. C. Vásquez, *Applied and environmental microbiology*, 2014, **80**, 7061-7070.
14. M. E. Castro, R. Molina, W. Díaz, S. E. Pichuantes and C. C. Vasquez, *Biochemical and biophysical research communications*, 2008, **375**, 91-94.
15. V. Tremaroli, M. L. Workentine, A. M. Weljie, H. J. Vogel, H. Ceri, C. Viti, E. Tatti, P. Zhang, A. P. Hynes, R. J. Turner and D. Zannoni, *Applied and environmental microbiology*, 2009, **75**, 719-728.
16. W. Zhang, L. Chen and D. Liu, *Applied microbiology and biotechnology*, 2012, **93**, 1305-1314.
17. S. Koc, B. Kabatas and B. Icgen, *Bulletin of environmental contamination and toxicology*, 2013, **91**, 177-183.
18. D. H. Nies, *Extremophiles*, 2000, **4**, 77-82.
19. T. von Rozycki and D. H. Nies, *Antonie van Leeuwenhoek*, 2009, **96**, 115-139.
20. D. Nies, M. Mergeay, B. Friedrich and H. G. Schlegel, *Journal of bacteriology*, 1987, **169**, 4865-4868.
21. R. J. Turner, Y. Hou, J. H. Weiner and D. E. Taylor, *Journal of bacteriology*, 1992, **174**, 3092-3094.
22. C. Rademacher, M. C. Hoffmann, J. W. Lackmann, R. Moser, Y. Pfander, S. Leimkuhler, F. Narberhaus and B. Masepohl, *Biometals : an international journal on the role of metal ions in biology, biochemistry, and medicine*, 2012, **25**, 995-1008.
23. A. Camacho, C. Rochera, R. Hennebelle, C. Ferrari and A. Quesada, *The Science of the total environment*, 2015, **509-510**, 145-153.
24. C. Vodopivez, A. Curtosi, E. Villaamil, P. Smichowski, E. Pelletier and W. P. Mac Cormack, *The Science of the total environment*, 2015, **502**, 375-384.
25. R. Ebinghaus, H. H. Kock, C. Temme, J. W. Einax, A. G. Lowe, A. Richter, J. P. Burrows and W. H. Schroeder, *Environmental science & technology*, 2002, **36**, 1238-1244.
26. H. von Waldow, M. MacLeod, K. Jones, M. Scheringer and K. Hungerbuhler, *Environmental science & technology*, 2010, **44**, 6183-6188.
27. S. Mangano, L. Michaud, C. Caruso and A. Lo Giudice, *Polar Biol*, 2014, **37**, 227-235.
28. M. J. De Souza, P. A. Loka Bharathi, S. Nair and D. Chandramohan, *Biometals*, 2007, **20**, 821-828.
29. F. A. Arenas, B. Pugin, N. A. Henríquez, M. A. Arenas-Salinas, W. A. Díaz-Vásquez, M. F. Pozo, C. M. Muñoz, T. G. Chasteen, J. M. Pérez-Donoso and C. C. Vásquez, *Polar Science*, 2014, **8**, 40-52.
30. W. G. Weisburg, S. M. Barns, D. A. Pelletier and D. J. Lane, *Journal of bacteriology*, 1991, **173**, 697-703.
31. A. D. Felske, W. Fehr, B. V. Pauling, H. von Canstein and I. Wagner-Dobler, *BMC microbiology*, 2003, **3**, 22.
32. N. Saitou and M. Nei, *Molecular biology and evolution*, 1987, **4**, 406-425.
33. J. Felsenstein, *The American Naturalist*, 1985, **125**, 1-15.
34. K. Tamura, G. Stecher, D. Peterson, A. Filipski and S. Kumar, *Molecular biology and evolution*, 2013, **30**, 2725-2729.
35. M. M. Bradford, *Analytical biochemistry*, 1976, **72**, 248-254.

36. K. J. Livak and T. D. Schmittgen, *Methods*, 2001, **25**, 402-408.

37. J. H. Yoon, C. H. Lee, S. H. Yeo and T. K. Oh, *International Journal of Systematic and Evolutionary Microbiology*, 2005, **55**, 1007-1013.

38. S. M. Andersen, K. Johnsen, J. Sorensen, P. Nielsen and C. S. Jacobsen, *International Journal of Systematic and Evolutionary Microbiology*, 2000, **50**, 1957-1964.

39. R. J. Turner, J. H. Weiner and D. E. Taylor, *Microbiol-Uk*, 1995, **141**, 3133-3140.

40. S. Verhille, N. Baida, F. Dabboussi, D. Izard and H. Leclerc, *Systematic and applied microbiology*, 1999, **22**, 45-58.

41. V. Subramanian, T. N. Liu, W. K. Yeh, C. M. Serdar, L. P. Wackett and D. T. Gibson, *Journal of Biological Chemistry*, 1985, **260**, 2355-2363.

42. T. A. Vishnivetskaya, M. A. Petrova, J. Urbance, M. Ponder, C. L. Moyer, D. A. Gilichinsky and J. M. Tiedje, *Astrobiology*, 2006, **6**, 400-414.

43. L. A. Romanenko, A. M. Lysenko, M. Rohde, V. V. Mikhailov and E. Stackebrandt, *International Journal of Systematic and Evolutionary Microbiology*, 2004, **54**, 1741-1745.

44. A. Heuchert, F. O. Glockner, R. Amann and U. Fischer, *Systematic and applied microbiology*, 2004, **27**, 399-406.

45. A. M. Osborn, K. D. Bruce, P. Strike and D. A. Ritchie, *FEMS microbiology reviews*, 1997, **19**, 239-262.

46. G. Kholodii and E. Bogdanova, *Genetica*, 2002, **115**, 233-241.

47. G. Y. Kholodii, O. V. Yurieva, Z. Gorlenko, S. Z. Mindlin, I. A. Bass, O. L. Lomovskaya, A. V. Kopteva and V. G. Nikiforov, *Microbiology*, 1997, **143**, 2549-2556.

48. G. Kholodii, O. Yurieva, S. Mindlin, Z. Gorlenko, V. Rybochkin and V. Nikiforov, *Research in microbiology*, 2000, **151**, 291-302.

49. G. Kholodii, S. Z. Mindlin, M. Gorlenko Zh, I. A. Bass, E. S. Kaliaeva and V. G. Nikiforov, *Genetika*, 2000, **36**, 459-469.

50. H. Kinoshita, Y. Sohma, F. Ohtake, M. Ishida, Y. Kawai, H. Kitazawa, T. Saito and K. Kimura, *Research in microbiology*, 2013, **164**, 701-709.

51. C. Cervantes-Vega, J. Chavez, N. A. Córdova, P. de la Mora and J. Amador Velasco, *Microbios*, 1986, **48**, 159-163.

52. R. J. Turner, Y. Aharonowitz, J. H. Weiner and D. E. Taylor, *Canadian journal of microbiology*, 2001, **47**, 33-40.

53. D. E. Fuentes, E. L. Fuentes, M. E. Castro, J. M. Pérez, M. A. Araya, T. G. Chasteen, S. E. Pichuantes and C. C. Vasquez, *Journal of bacteriology*, 2007, **189**, 8953-8960.

54. C. C. Vasquez, C. P. Saavedra, C. A. Loyola, M. A. Araya and S. Pichuantes, *Current microbiology*, 2001, **43**, 418-423.

55. C. P. Saavedra, M. V. Encinas, M. A. Araya, J. M. Perez, J. C. Tantalean, D. E. Fuentes, I. L. Calderon, S. E. Pichuantes and C. C. Vasquez, *Biochimie*, 2004, **86**, 481-485.

56. T. G. Chasteen and R. Bentley, *Chemical reviews*, 2003, **103**, 1-25.

57. K. Smalla, A. S. Haines, K. Jones, E. Krogerrecklenfort, H. Heuer, M. Schloter and C. M. Thomas, *Applied and environmental microbiology*, 2006, **72**, 7253-7259.

58. B. Marteyn, S. Sakr, S. Farci, M. Bedhomme, S. Chardonnet, P. Decottignies, S. D. Lemaire, C. Cassier-Chauvat and F. Chauvat, *Journal of bacteriology*, 2013, **195**, 4138-4145.

59. A. Onnis-Hayden, H. Weng, M. He, S. Hansen, V. Ilyin, K. Lewis and A. Z. Guc, *Environmental science & technology*, 2009, **43**, 4574-4581.

60. M. Rafati-Rahimzadeh, M. Rafati-Rahimzadeh, S. Kazemi and A. A. Moghadamnia, *Daru : journal of Faculty of Pharmacy, Tehran University of Medical Sciences*, 2014, **22**, 46.

61. S. Park and R. L. Ely, *Applied and environmental microbiology*, 2008, **74**, 5475-5482.

62. S. Park and R. L. Ely, *Archives of microbiology*, 2008, **189**, 541-548.

63. M. Kiyono, K. Miyahara, Y. Sone, H. Pan-Hou, S. Uraguchi, R. Nakamura and K. Sakabe, *Applied microbiology and biotechnology*, 2010, **86**, 753-759.

64. D. Raimunda, T. Padilla-Benavides, S. Vogt, S. Boutigny, K. N. Tomkinson, L. A. Finney and J. M. Arguello, *Metallomics : integrated biometal science*, 2013, **5**, 144-151.

65. A. S. Gort, D. M. Ferber and J. A. Imlay, *Molecular microbiology*, 1999, **32**, 179-191.

66. R. Hengge-Aronis, *Microbiology and molecular biology reviews*, 2002, **66**, 373-395, table of contents.

67. P. Banjerdkij, P. Vattanaviboon and S. Mongkolsuk, *Current microbiology*, 2003, **47**, 260-262.

68. P. Banjerdkij, P. Vattanaviboon and S. Mongkolsuk, *Applied and environmental microbiology*, 2005, **71**, 1843-1849.

69. O. Cantoni, S. Hussain, A. Guidarelli and F. Cattabeni, *Mutation research*, 1994, **324**, 1-6.

70. Z. P. Cakar, C. Alkim, B. Turanli, N. Tokman, S. Akman, M. Sarikaya, C. Tamerler, L. Benbadis and J. M. Francois, *Journal of biotechnology*, 2009, **143**, 130-138.

71. M. Sen, U. Yilmaz, A. Baysal, S. Akman and Z. P. Cakar, *Antonie van Leeuwenhoek*, 2011, **99**, 825-835.

72. A. Toptchieva, G. Sisson, L. J. Bryden, D. E. Taylor and P. S. Hoffman, *Microbiology*, 2003, **149**, 1285-1295.